Mon. Not. R. Astron. Soc. **000**, 000–000 (1993)

The Cambridge-Cambridge X-ray Serendipity Survey: I X-ray luminous galaxies

B.J.Boyle[1], R.G.McMahon[1], B.J.Wilkes[2], M.Elvis[2]

[1] *Institute of Astronomy, University of Cambridge, Madingley Road, Cambridge, CB3 0HA*
[2] *Center for Astrophysics, 60 Garden St, Cambridge MA 21260, USA.*

ABSTRACT

We report on the first results obtained from a new optical identification program of 123 faint X-ray sources with $S(0.5\text{–}2\,\mathrm{keV}) > 2 \times 10^{-14}\,\mathrm{erg\,s^{-1}\,cm^{-2}}$ serendipitously detected in ROSAT PSPC pointed observations. We have spectroscopically identified the optical counterparts to more than 100 sources in this survey. Although the majority of the sample (68 objects) are QSOs, we have also identified 12 narrow emission line galaxies which have extreme X-ray luminosities ($10^{42} < L_{\mathrm{X}} < 10^{43.5}\,\mathrm{erg\,s^{-1}}$). Subsequent spectroscopy reveals then to be a mixture of star-burst galaxies and Seyfert 2 galaxies in approximately equal numbers. Combined with potentially similar objects identified in the Einstein Extended Medium Sensitivity Survey, these X-ray luminous galaxies exhibit a rate of cosmological evolution, $L_{\mathrm{X}} \propto (1+z)^{2.5\pm1.0}$, consistent with that derived for X-ray QSOs. This evolution, coupled with the steep slope determined for the faint end of the X-ray luminosity function ($\Phi(L_{\mathrm{X}}) \propto L_{\mathrm{X}}^{-1.9}$), implies that such objects could comprise 15–35 per cent of the soft (1-2 keV) X-ray background.

Key words: X-rays: general – galaxies: active – quasars: general

1 INTRODUCTION

The launch of ROSAT has provided a new opportunity to resolve the soft (0.5-2 keV) X-ray background (XRB) down to flux levels five times fainter than achieved with the deepest pointings performed by the *Einstein* satellite (Griffiths et al. 1992). At these levels ($S \sim 2 \times 10^{-15}\,\mathrm{erg\,s^{-1}\,cm^{-2}}$) almost 60 per cent of the XRB is resolved (Hasinger et al. 1993) and, at the current limit of the follow-up optical identification programs ($S \sim 4 \times 10^{-15}\mathrm{erg\,s^{-1}\,cm^{-2}}$, Georgantopoulos et al. 1994), QSOs account for the majority ($\sim 75\%$) of the extra-galactic sources. However, fluctuation analyses (Hasinger et al. 1993, Georgantopoulos et al. 1993) and differences between the X-ray spectra of QSOs and that of the background (Georgantopoulos et al. 1994) suggest that these QSOs are unlikely to contribute more than ~ 50 per cent of the 1 keV background and probably do not comprise more than ~ 20 per cent of the XRB at harder energies (2–10 keV), the energy range at which the XRB was first discovered (Giacconi et al. 1962). Indeed, at faint flux levels, $S < 10^{-14}\mathrm{erg\,s^{-1}\,cm^{-2}}$, the spectroscopic observations of Georgantopoulos et al. (1994) tentatively identify an increasingly large fraction of galaxies as counterparts to X-ray sources.

Unfortunately the low flux levels currently employed in both the X-ray and optical regimes make optical identification difficult and positional coincidence hard to establish conclusively (e.g. Georgantopoulos et al. 1994). By slightly increasing the flux limit and extending any survey over a wider area, it may be possible to identify the brighter members of any new class. We have therefore carried out an optical identification program of X-ray sources detected by ROSAT at a level intermediate in flux, $S(0.5-2\,\mathrm{keV}) = 2 \times 10^{-14}\mathrm{erg\,s^{-1}\,cm^{-2}}$, between the deepest ROSAT surveys and the Extended Medium Sensitivity Survey (EMSS, see Stocke et al. 1991) performed with the *Einstein* satellite at a flux limit $S(0.3-3.5\,\mathrm{keV}) \sim 1 \times 10^{-13}\mathrm{erg\,s^{-1}\,cm^{-2}}$. The sources in our survey were detected 'serendipitously' in existing PSPC fields available in the ROSAT archive, originally taken to study the X-ray properties of known targets (QSOs/CVs/galaxies). The optical counterparts of these X-ray sources were identified spectroscopically with the William Herschel Telescope (WHT). A full description of the survey and catalogue will appear elsewhere (McMahon et al. 1994, in preparation, hereafter M94). In this paper we report on the discovery of a significant number of narrow emission line galaxies in the survey. In Section 2 we briefly describe the selection of the X-ray sources, the optical identification procedure and the spectroscopic observations. We discuss our results in Section 3 and present our conclusions in Section 4.

2 OBSERVATIONS

2.1 X-ray source detection

Objects in the Cambridge-Cambridge ROSAT serendipity survey (CRSS) were detected as serendipitous X-ray

Table 1. Survey fields

Field Name	RA (J2000) Dec		Flux Limit	N_H
	h m s	° ′ ″	($\mathrm{erg\,s^{-1}\,cm^{-2}}$)	($10^{20}\,\mathrm{cm^{-2}}$)
MKN335	00 08 19.2	20 41 24	2.0×10^{-14}	4.1
PG0027	00 30 05.7	26 17 22	2.0×10^{-14}	3.9
OQ208	14 07 00.4	28 27 14	2.0×10^{-14}	1.4
PG1411	14 13 48.4	44 00 14	2.0×10^{-14}	1.2
Q1413+11	14 15 46.3	11 29 44	2.0×10^{-14}	1.8
3C298	14 19 08.2	06 28 35	2.0×10^{-13}	2.1
OQ530	14 19 46.6	54 23 14	2.0×10^{-14}	1.3
PG1426	14 29 06.6	01 17 06	2.5×10^{-14}	2.7
4U1417+42	14 28 32.5	42 40 25	3.0×10^{-14}	1.4
PG1512	15 14 43.0	36 50 51	4.0×10^{-14}	1.4
NGC5907	15 15 52.9	56 19 33	2.0×10^{-14}	1.4
PG1543	15 45 30.1	48 46 12	3.0×10^{-14}	1.6
MS1603.6	16 05 46.0	25 51 44	2.0×10^{-14}	4.6
E1615+061	16 17 45.5	06 03 55	3.5×10^{-14}	4.6
3C334	16 20 21.8	17 36 22	5.0×10^{-14}	4.1
MARK501	16 53 52.2	39 45 36	7.5×10^{-14}	1.7
PG1704	17 04 41.5	60 44 28	2.0×10^{-14}	2.3
PG2233	22 36 07.7	13 43 55	5.0×10^{-14}	4.9
PKS2247	22 50 25.3	14 19 53	4.0×10^{-14}	4.8
HR8905	23 25 22.1	23 24 13	3.0×10^{-14}	4.7

sources in high galactic latitude ($b^{II} > 30°$) PSPC fields available in the ROSAT archive prior to 1993 July. All selected fields had exposure times greater than 6000 s. X-ray sources were detected on 20 PSPC fields with $14^h < RA < 1^h$ and $\delta > 0°$. On each field source detection was limited to within 15 arcmin off-axis in order to maintain relatively high positional accuracy for the sources (1σ error $\simeq$ 8 arcsec) and to avoid obscuration by the rib support structure at larger off-axis angles. Sources were detected using the IMAGES algorithm written by Dr Mike Irwin (now available as PISA in the STARLINK software collection), which detected sources with four or more 15-arcsec pixels lying 1.5 times the rms noise level above the background. Source detection on each field was limited to a flux level $S(0.5-2\,\mathrm{keV}) > 2\times10^{-14}\,\mathrm{erg\,s^{-1}\,cm^{-2}}$, significantly greater than the faintest flux detectable even on the fields with the shortest exposures. Source fluxes were measured using a fixed 2.5 pixel radius aperture. Background subtraction was made using a single level for the whole field (typically $< 0.3\,\mathrm{counts\,pixel^{-1}}$), determined from a fit to the histogram of pixel values within the 15-arcmin radius region. On than half of the fields in this analysis (11), the spectroscopic identification is 90 per cent complete to the flux limit $S(0.5-2\,\mathrm{keV}) > 2\times10^{-14}\,\mathrm{erg\,s^{-1}\,cm^{-2}}$. On the other fields (principally the shorter exposure fields), we subsequently imposed a brighter flux limit to ensure a similar level of spectroscopic completeness on these fields. The revised area coverage as a function of X-ray flux limit in the $0.5-2$ keV passband is given in Table 1. A total of 123 serendipitous sources were identified over the 20 PSPC fields used in this analysis.

2.2 Optical Identification

In order to search for optical counterparts, the measured X,Y positions for the X-ray sources were transformed to RA and Dec using their offset from the central 'target' source in each PSPC field (usually a QSO) whose optical position was known to 1-arcsec accuracy. APM measurements of Palomar Observatory Sky Survey (POSS) O and E plates (McMahon and Irwin 1994) were then used to provide a list of optical counterparts found within 20 arcsec of each source. Out to 20 arcsec, 112 out of 123 X-ray sources (91 per cent) had at least one optical counterpart identified to the limit of the POSS plates ($O < 21.5$ mag, $E < 20$ mag). The 20 arcsec radius represents 2.5 times the observed width of the X-ray to optical positional cross-correlation function (Fig. 1(a)). The mean $O-E$ colour of these counterparts is much bluer than the overall colour distribution (Fig. 1(b)), demonstrating the counterparts are dominated by QSOs ($O-E \sim 1$ mag, McMahon 1991). The X-ray source positions were subsequently revised to give a zero mean positional offset in each field between the X-ray and optical positions of sources with a blue ($O-E < 1.2$ mag) optical counterpart. However, this only changed the nearest optical counterpart in 5 per cent of the total sample. As can be seen from Fig. 1(a), a significant number of optical images ($\sim$ 35 per cent) identified within 20 arcsec will be chance coincidences, giving rise to multiple optical counterparts for some X-ray sources. For sources with more than one optical counterpart, spectroscopy was carried out in strict order of increasing separation between the X-ray position and optical counterpart until a plausible candidate (e.g. QSO, M star) was identified. In all but 10 cases the closest object

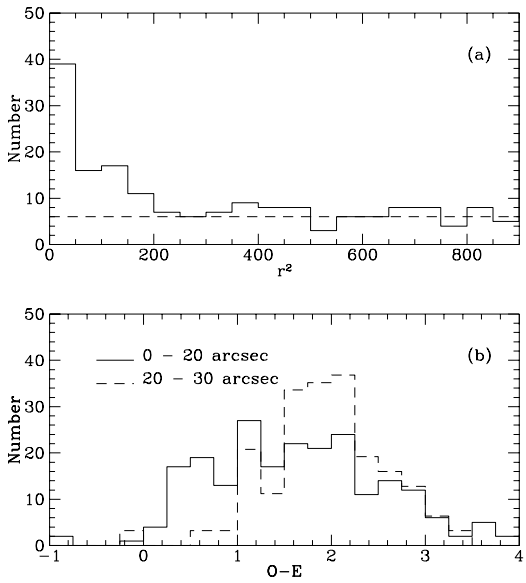

Figure 1(a). Number of optical identifications as a function of separation from X-ray source position. Bins are in units of separation^2 (arcsec^2) so the level of chance coincidences is constant (dotted line). **Figure 1(b).** $O-E$ colour distributions for the optical counterparts within 20 arcmin of the X-ray position and the overall colour distribution of the field, based on the normalised distribution of colours for optical identifications lying $20-30$ arcsec from the X-ray sources.

turned out to be the correct identification.

2.3 Optical Spectroscopy

Low resolution ($\sim$ 6Å) spectroscopy was obtained for the optical counterparts with the ISIS double arm spectrograph at the WHT on the nights of 1993 June 19–22. ISIS was operated with 158 lines/mm gratings in the blue and red arms (a dichroic filter was used to split the light at 5400Å), with the Tektronix and EEV CCDs as the detectors in the blue and red arms respectively giving an overall instrumental resolution of 2.9Å/pixel. Throughout the run the seeing was $\sim$ 1 arcsec, and most of the observations were made with a 1.5 arcsec slit. In these conditions, exposure times of 300–1200 sec were sufficient to yield an adequate signal-to-noise ratio ($\sim$ 15) in the spectra of the optical candidates ($19 < O < 21$). Spectra for 118 optical candidates were obtained, resulting in a positive optical identification for 107 of the 123 X-ray sources in the CRSS (including 3 previously known QSOs). An additional 2 bright ($O < 12$ mag) stellar optical counterparts were not observed, but if they are assumed to be galactic stars, the identification rate for the survey is 89 per cent. Of the remaining 14 unidentified X-ray sources, 11 had no optical counterpart within 20 arcsec of the X-ray position on the PSS, 1 optical counterpart had an inconclusive, low signal-to-noise spectrum and a further optical counterpart was not observed due to lack of time. A KS test performed on the X-ray flux distribution of both the identified and unidentified sources revealed no significant differences between in the flux distribution for the two samples at the 95 per cent confidence level. To account for this incompleteness, in the analysis below we have therefore multiplied the total area surveyed at each X-ray flux limit (see Table 1) by 0.89 to yield an effective survey area.

3 X-RAY GALAXIES

3.1 General Properties

The majority of the objects identified were QSOs (68), classified from the presence of broad ($> 1000\,\mathrm{km\,s^{-1}}$) emission lines. Full details of the properties of the QSO population (e.g. evolution, luminosity function) will be discussed by M94.

We also identified 12 narrow emission line galaxies with optical magnitudes in the range $17 < 0 < 21$. The criterion for inclusion in this class was a measured Hα full width half maximum (FWHM) of $< 1000\,\mathrm{km\,s^{-1}}$. The limit clearly marks the division between broad and narrow emission lines in the CRSS survey (see Fig. 2). The discovery spectra for all these galaxies are plotted in Fig. 3 and their names, positions, redshifts, $0.5-2$ keV fluxes and luminosities are given in Table 1. Luminosities were derived assuming $q_0 = 0.5$, $H_0 = 50\,\mathrm{km\,s^{-1}Mpc^{-1}}$ and a X-ray spectral index $\alpha_X = 1.0$. The X-ray luminosities for these galaxies lie in the range $10^{42} < L_X < 10^{43.5}\,\mathrm{erg\,s^{-1}}$, one to two orders of magnitude more luminous than late-type galaxies (Fabbiano 1989), whose optical spectra these objects most closely resemble. All the X-ray images for these galaxies are consistent with a point source, ruling out any significant contribution to the X-ray luminosity from extended cluster emission at the typical redshift ($z \sim 0.2$) of the sample.

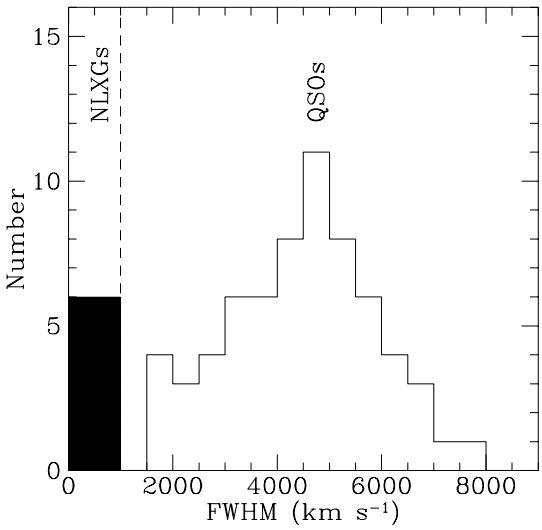

Figure 2. Histogram of emission line full width half maxima (FWHM) for the QSOs and NLXGs in the CRSS. The classification criterion used to identify NLXGs (FWHM $< 1000\,\mathrm{km\,s^{-1}}$) is indicated by the dashed line.

It is unlikely that galaxies have been identified merely by chance positional coincidence. All galaxies were found within 10 arcsec of the X-ray source position. Based on the mean surface density of optical counterparts to the plate limit (see Fig. 1(a)) we expect only 15 per cent of the X-ray sources to have a spurious optical counterpart at this separation. Of these chance coincidences, approximately half will be galaxies (based on the relative numbers of stars and galaxies identified at the PSS plate limit) and, of these galaxies, $\sim 20-30$ per cent will exhibit emission lines (based on the relative number of emission line galaxies at this magnitude limit, Broadhurst et al. 1988). Thus only $\sim 1-2$ per cent of the total sample ($\sim 1-2$ X-ray sources) will have a positional coincidence (at < 10 arcsec) with an emission line galaxy. An even smaller fraction will exhibit the high [OIII]/[OII] emission line ratios observed for galaxies in this sample (see below) and thus we consider it likely that the vast majority, if not all, of these galaxies are the true counterparts of the X-ray sources.

The galaxies exhibit emission lines of [OII] λ3727, Hβ, [OIII]$\lambda\lambda$4959, 5007, [NII] $\lambda\lambda$6548, 6583, Hα and [S II]$\lambda\lambda$6716, 6731, typical of many late-type galaxies identified in field galaxy surveys at this optical magnitude (Broadhurst et al. 1988). However, the observed emission line ratios, in particular the strength of [OIII] relative to [OII] ($1 <$ [OIII]λ5007/[OII]λ3727 < 4), indicates a much higher state of ionisation than is normally observed for field galaxies.

Table 2. NLXGs identified in the CRSS

Name	Survey Name	RA (2000) Dec						$S(0.5-2\,\mathrm{keV})$	z	$L(0.5-2\,\mathrm{keV})$	$\frac{\mathrm{I([OIII])}}{\mathrm{I(H}\beta\mathrm{)}}$	$\frac{\mathrm{I([NII])}}{\mathrm{I(H}\alpha\mathrm{)}}$	ID
		h	m	s	°	′	″	$(\mathrm{erg\,s^{-1}\,cm^{-2}})$		$(\mathrm{erg\,s^{-1}})$			
CRSS0009.0+2041	MKN335:08	00	09	01.7	20	41	36	2.0×10^{-14}	0.189	3.4×10^{42}		0.5	HII?
CRSS0030.2+2611	PG0027:10	00	30	17.4	26	11	38	5.1×10^{-14}	0.077	1.7×10^{42}	0.2	0.5	HII
CRSS0030.7+2629	PG0027:19	00	30	47.9	26	29	34	2.0×10^{-14}	0.246	5.9×10^{42}		0.9	Sy 2
CRSS1406.7+2838	OQ208:43	14	06	47.9	28	38	53	2.8×10^{-14}	0.331	1.5×10^{43}		0.3	HII?
CRSS1412.5+4355	PG1411:14	14	12	31.6	43	55	36	2.2×10^{-13}	0.094	8.9×10^{42}	3.6	0.7	Sy 2
CRSS1413.3+4405	PG1411:22	14	13	19.9	44	05	34	5.2×10^{-14}	0.136	4.5×10^{42}	7.6	0.8	Sy 2
CRSS1415.0+4402	PG1411:19	14	15	00.1	44	02	08	2.9×10^{-14}	0.136	2.5×10^{42}	7.9	0.8	Sy 2
CRSS1429.0+0120	PG1426:03	14	29	04.7	01	20	17	4.3×10^{-14}	0.102	2.0×10^{42}	1.5	0.6	Sy 2
CRSS1514.4+5627	N5907:15	15	14	29.6	56	27	07	3.7×10^{-14}	0.446	3.8×10^{43}			–
CRSS1605.6+2543	MS1603:07	16	05	39.9	25	43	10	4.4×10^{-14}	0.278	1.7×10^{43}	0.5	0.4	HII
CRSS1605.9+2554	MS1603:16	16	05	58.7	25	54	08	4.1×10^{-14}	0.151	4.4×10^{42}			–
CRSS1705.3+6049	PG1704:11	17	05	18.3	60	G49	54	2.7×10^{-14}	0.572	4.6×10^{43}	>2		Sy 2?

Table 3. NLXGs observed in the EMSS.

Name	z	$L(0.3-3.5\,\mathrm{keV})$ $(\mathrm{erg\,s^{-1}})$	$\frac{\mathrm{I([OIII])}}{\mathrm{I(H}\beta\mathrm{)}}$	$\frac{\mathrm{I([NII])}}{\mathrm{I(H}\alpha\mathrm{)}}$	ID
MS1252.4+0457	0.158	2.6×10^{43}	0.58	0.88	Sy 2
MS1334.6+0351	0.136	2.4×10^{43}	3.30	1.05	Sy 2
MS1412.8+1320	0.139	2.2×10^{43}	0.58	0.36	HII
MS1414.8−1247	0.198	1.3×10^{44}	2.08	0.33	HII
MS1555.1+4522	0.181	6.9×10^{43}	7.05	0.91	Sy 2
MS1614.1+3239	0.118	1.7×10^{43}	>10	1.23	Sy 2
MS2044.1+3532	0.183	3.7×10^{43}	2.7	0.52	Sy 2/HII

We have managed to obtain a more accurate classification for 10 of the narrow-line X-ray galaxies (NLXGs) using subsequent higher resolution (1.5 Å), higher signal-to-noise ISIS spectra of the redshifted Hα and Hβ regions in these objects. These were obtained during an observing run on 1994 June 9-10 and during service time on 1993 September 20. A detailed discussion of these spectra will be presented elsewhere (Boyle et al., in preparation), but a classification based on the relative strengths of the Hβ, [OIII]λ5007, [OI]λ6300, Hα and [NII]λ6583 lines using the schemes of Baldwin, Philips & Terlevich (1981) and Filippenko & Terlevich (1992) reveals that the sample is composed of approximately equal numbers of starburst-like galaxies and Seyfert 2-like galaxies, although many objects lie close to the transition regions in the classification schemes used. Emission line ratios and classifications for these objects are presented in Table 2. The measured FWHM for the Balmer lines in these spectra lie in the range $180\mathrm{km\,s^{-1}} < \mathrm{FWHM} < 450\mathrm{km\,s^{-1}}$, confirming their original identification as narrow-lined objects, and distinct from broad-lined QSOs. However, as many as half the sample may exhibit weak broad emission ($\mathrm{FWHM} > 1000\mathrm{km\,s^{-1}}$) at the base of H$\alpha$, although this is very much dependent on the adopted emission line profile used to fit the more prominent narrow emission lines. In only one case (CRSS1413+4405) is there clear evidence for a residual weak broad component ($\mathrm{FWHM}\sim 6000\mathrm{km\,s^{-1}}$), even after logarithmic line profiles have been used to fit the narrow emission lines.

Similar examples of X-ray luminous ($10^{42} < L_{\mathrm{X}} < 10^{43}\,\mathrm{erg\,s^{-1}}$) narrow emission line galaxies were also identified at low redshift ($z \lesssim 0.2$) in the EMSS by Stocke et al. (1991). Since the emission line galaxies fulfilled the criterion that [OIII]λ5007 >[OII]λ3727, they were classified as AGN without exhibiting any broad emission lines. Based on the list of 'ambiguous' sources listed in tables 8 and 10 of Stocke et al. (1991), it is possible that up to 31 objects classified as AGN in the EMSS could be similar to the types of NLXGs identified in the CRSS. We observed 7 of these objects with ISIS at 1.5 Å resolution during the WHT run on 1994 June 9-10 and found that the FWHM of the Hα and Hβ lines lay in the range 200–600km s^{-1}, although, as was the case for the CRSS objects, the presence of weak broad lines was difficult to establish due to uncertainties in profile fitting the wings of the narrow emission lines. The measured emission line ratios and corresponding classifications for these seven EMSS objects are given in Table 3. Despite the small numbers of objects involved, the relative numbers of starburst-like spectra and Seyfert 2-like spectra seem approximately similar to those identified in the CRSS. Moreover, these numbers agree with those found from a similar spectroscopic classification of the ambiguous EMSS sources performed by Fruscione, Griffiths and Mackenty (1993). Although it would appear unlikely that the NLXGs in either the CRSS or EMSS form a homogeneous group (although most lie close to the classification boundary between starburst galaxies and Seyfert 2s), an overall estimate of their total space density and evolution can be used to provide a useful upper limit to the contribution of NLXGs (starburst + Seyfert 2) to the 1-2 keV XRB. by We have therefore combined the EMSS 'ambiguous' sources with the CRSS NLXGs to give a total sample of 43 objects, which will be used as the basis for the analysis below.

3.2 Evolution

The NLXG fraction in the total X-ray source counts (including non-extragalatic sources) increases with flux limit (4 per cent in the EMSS, $S(0.3-3.5\mathrm{keV}) > 1\times10^{-13}\mathrm{erg\,s^{-1}\,cm^{-2}}$ and 10 per cent in the CRSS, $S(0.5-2\mathrm{keV}) > 2\times10^{-14}\mathrm{erg\,s^{-1}\,cm^{-2}}$) in a similar manner to QSOs. To establish whether this was due to cosmological evolution,

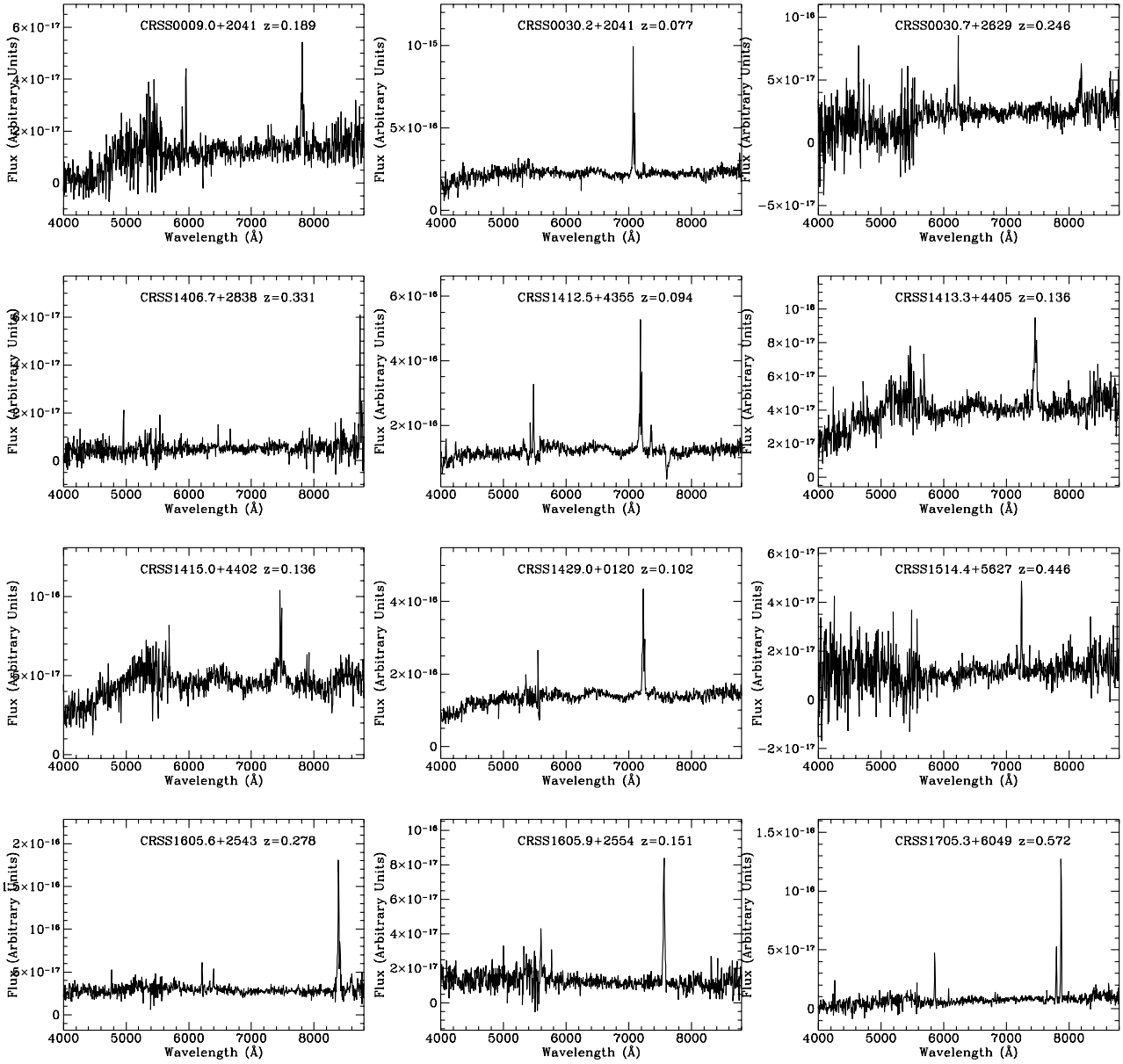

Figure 3. Low resolution (10Å) spectra for all 12 narrow emission line galaxies identified in the CRSS.

we calculated the $< V_e/V_a >$ statistic (Avni and Bachall 1980) for the 43 NLXGs in the EMSS and CRSS. We first converted the 0.5-2 keV ROSAT fluxes to the *Einstein* band assuming $S(0.3-3.5\,\mathrm{keV}) = 1.8 \times S(0.5-2\,\mathrm{keV})$, appropriate for an X-ray spectral index $0.8 < \alpha_X < 1.5$ (Boyle et al. 1993). For $q_0 = 0.5$ we obtained a value of $< V_e/V_a >= 0.72 \pm 0.04$, more than 5σ higher than the no evolution value of 0.5.

Having confirmed that the NLXG sample exhibits significant cosmolgical evolution, we then used the maximum likelihood technique to obtain a 'best-fit' parametric representation of the evolution and luminosity function (LF) of this sample. We adopted a two power model for the NLXG LF, also found to fit the QSO X-ray LF (Boyle et al. 1993):

$$\Phi(L_X) = \Phi^* L_{X_{44}}^{-\gamma_1} \qquad L_X < L_X^*(z=0)$$

$$\Phi(L_X) = \frac{\Phi^*}{L_{X_{44}}^{\gamma_1-\gamma_2}} L_{X_{44}}^{-\gamma_2} \qquad L_X > L_X^*(z=0)$$

where Φ^* is the normalization of the LF and γ_1, γ_2 are the slopes of the faint and bright end of the XLF. $L_{X_{44}}$ is 0.3-3.5 keV X-ray luminosity expressed in units of $10^{44}\,\mathrm{erg\,s^{-1}}$. The evolution of the NLXG LF was also assumed to have the same form as that adopted for the QSOs; namely a $(1+z)$

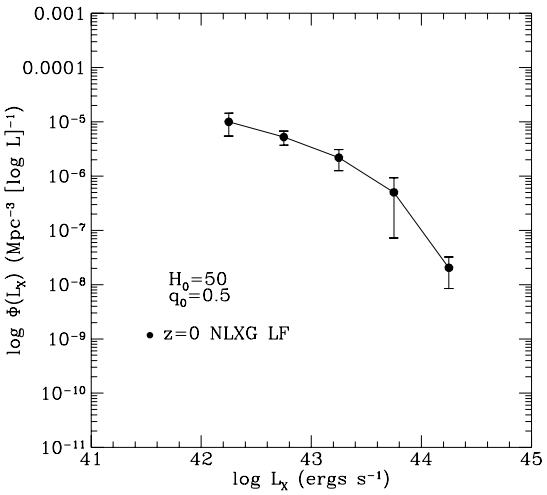

Figure 4. The de-evolved X-ray luminosity function for the X-ray luminous galaxies identified in the EMSS and CRSS.

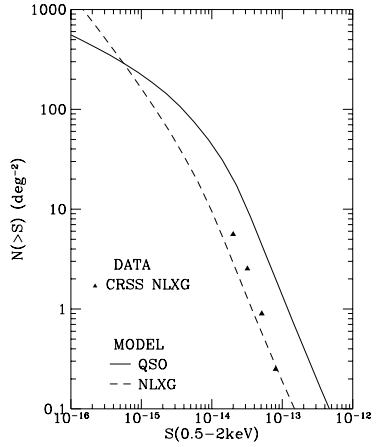

Figure 5. The number-flux relation for NLXGs in the CRSS (triangles). The predicted number-flux relation for X-ray galaxies based on the evolution model described in the text is denoted by the dotted line. The solid line illustrates the predicted number-flux relation for QSOs based on evolution model U of Boyle et al. (1994).

power-law evolution in the 'break' luminosity, $L^*_{\rm X}(z)$:

$$L^*_{\rm X}(z) = L^*_{\rm X}(0)\ (1+z)^k$$

Throughout this analysis we adopt a spectral index $\alpha_{\rm X} = 1$. Although it is slightly harder than the mean spectral index derived for the NLXGs in the CRSS ($\alpha_{\rm X} = 1.2$, Cilegi et al., in preparation), by using this value we can directly compare our results with those for X-ray selected QSOs (Maccacaro et al. 1991, Boyle et al. 1993, 1994) also obtained for $\alpha_{\rm X} = 1$. Nevertheless, the effect of spectral index of the derived power-law evolution is extremely straightforward, viz. any change to the adopted QSO spectral index, $\alpha_{\rm X}$, results in an identical change in the derived value of the evolution parameter k.

From the maximum likelihood analysis we obtain the following best-fit parameter values: $\gamma_1 = 1.9 \pm 0.25$, $\gamma_2 = 3.8 \pm 0.2$, $L^*_{\rm X}(0) = 10^{43.21\pm0.2}{\rm erg\,s^{-1}}$, $k = 2.5 \pm 1.0$ and $\Phi^* = 1.6 \times 10^{-7}\,{\rm Mpc^{-3}}(10^{44}\,{\rm erg\,s^{-1}})^{-1}$. This model was an acceptable fit to the data with a KS probability of greater than 10 per cent. Although dominated by a large error (caused by the small redshift range of the sample), the derived rate of evolution for these objects is consistent with that obtained by Boyle et al. (1994) for X-ray QSOs ($k = 3.17$) after the exclusion of the 31 EMSS 'ambiguous' sources (model U in Boyle et al. 1994). A binned version of the de-evolved $z = 0$ LF is plotted in Fig. 4. The observed and predicted number-flux relation for the NLXGs is plotted in Fig. 5, together with the predicted QSO number-flux relation based on model U in Boyle et al. (1994). Both models are integrated out to $z = 4$, with no evolution beyond $z_{\rm max} = 2$. These models predict that the QSOs dominate the X-ray source counts until $S(0.3-3.5{\rm keV}) \sim 2 \times 10^{-16}{\rm erg\,s^{-1}\,cm^{-2}}$, beyond which NLXGs become the dominant population.

3.3 The X-ray Background

To estimate the specific intensity due to NLXGs, we integrate over the 0.3 − 3.5 keV LF:

$$I_{\rm NLXG} = \frac{c}{4\pi H_0} \int_{L_{\rm X_{min}}}^{L_{\rm X_{max}}} \int_{z_{\rm min}}^{z_{\rm max}} \frac{L_{\rm X}\Phi(L_{\rm X})(1+z)^k}{(1+2q_0z)^{0.5}(1+z)^{2+\alpha_{\rm X}}} dz dL$$

where we have chosen our limits to be $L_{\rm X_{min}} = 10^{39}\,{\rm erg\,s^{-1}}$, $L_{\rm X_{max}} = 10^{47}\,{\rm erg\,s^{-1}}$, $z_{\rm min} = 0$ and $z_{\rm max} = 4$. We use the specific intensity of the extra-galactic background in the 1 − 2 keV energy range derived by Hasinger et al. (1993), $I_{\rm XRB}$(1-2 keV) $= 1.25 \times 10^{-8}\,{\rm erg\,cm^{-2}s^{-1}sr^{-1}}$. Assuming a spectral index of $\alpha_{\rm X} = 1$, the specific intensity derived for NLXG in the 0.3 − 3.5 keV band is multiplied by 0.28 to obtain the specific intensity in the 1 − 2 keV band. Note that the fractional contribution of NLXGs to the XRB computed by this method is insensitive to the choice of spectral index, since any increase in the adopted spectral index will be precisely cancelled out in the above equation by the corresponding increase in the evolution parameter k (see above).

For our best-fit model we obtain a specific intensity $I_{\rm NLXG}(1-2\,{\rm keV}) = 2.4 \times 10^{-9}\,{\rm erg\,cm^{-2}s^{-1}sr^{-1}}$, corresponding to a contribution to the XRB of 16 per cent. However, this model assumes that the power law evolution continues unchecked until $z = 4$. A more realistic model would include a maximum redshift $z_{\rm max}$ beyond which the evolution 'switches off' and the comoving space density of QSOs remains constant. Adopting $z_{\rm max} = 2$, consistent with the X-ray evolution of QSOs (Boyle et al. 1993), we derive an overall contribution of 14 per cent. This implies that most of the contribution to the XRB from these galaxies comes from within $z < 2$. The contribution to the XRB from NLXGs with $L_{\rm X} > 10^{42}\,{\rm erg\,s^{-1}}$ (the minimum luminosity observed in our sample) is 6 per cent.

There are also significant uncertainties in the XRB calculation associated with the value of the 'best-fit' parameters. In the model with $z_{\rm max} = 2$ considered here, increasing

the evolution parameter to its 1σ upper limit, $k = 3.5$ results in a contribution of 32 per cent. However, the biggest uncertainty in the estimated contribution to the XRB is the slope of the faint end of the luminosity function. Although the best-estimate is $\gamma_1 = 1.89$, the value of $\gamma_2 = 2$ is within the 1σ error. With such a steep slope, $I_{\rm NLXG}$ does not converge and the derived contribution to the XRB is dependent on the lower luminosity limit adopted in the integration. For $L_{\rm X_{min}} = 10^{37}\,{\rm erg\,s^{-1}}$, a model with $k = 2.5$, $\gamma_1 = 2.0$ and $z_{\rm max} = 2$, the contribution more than doubles from 14 per cent to 37 per cent. Further decreasing the minimum luminosity in the limit of integration would increase the contribution to even higher values.

4 CONCLUSIONS

We have identified 12 X-ray luminous narrow emission line galaxies (NLXGs) based on a spectroscopic survey of 123 serendipitous ROSAT X-ray sources with $S(0.5-2{\rm keV}) > 2\times10^{-14}\,{\rm erg\,s^{-1}cm^{-2}}$. The X-ray luminosities of these galaxies range from $10^{42}-10^{43.5}\,{\rm erg\,s^{-1}}$, one to two orders of magnitude greater than observed for typical late type galaxies. Their optical spectra exhibit emission line ratios characteristic of high ionisation, and the sample appears to be composed of approximately equal numbers of starburst and Seyfert 2 galaxies. Coupled with a potentially similar class of objects in the EMSS, the NLXGs exhibit a rate of cosmological evolution, $L_{\rm X}\propto(1+z)^{2.6\pm1.0}$ similar to that derived for X-ray QSOs. The NLXG luminosity function exhibits the same two power law form as the QSO luminosity function, but with a steeper faint end slope. Extrapolation of the luminosity function and its evolution yields a predicted NLXG contribution to the $1-2\,{\rm keV}$ X-ray background of $15-35$ per cent, with NLXGs comprising the majority of the faint X-ray sources at $S(0.5-2{\rm keV}) < 2\times10^{-16}{\rm erg\,s^{-1}\,cm^{-2}}$. Further classification of the NLXGs in the EMSS and CRSS samples will enable luminosity functions to be derived for the different types of object that make up this heterogeneous class, but if the current relative numbers of starburst and Seyfert 2 galaxies observed are typical, then it suggests that both types of object contribute between 7 – 17 per cent of the 2 keV background.

ACKNOWLEDGMENTS

BJB and RGM acknowledge the receipt of Royal Society University Research Fellowships. We are indebted to Dr Mike Irwin for observing the two spectra obtained during spectroscopic service time on the William Herschel Telescope. BJB also acknowledges the support and hospitality of the Smithsonian Astrophysical Observatory. The X-ray data was obtained from the Leicester and Goddard ROSAT archives. This work was partially supported by NASA grants NAGW-2201 (LTSA) and NAS5-30934 (RSDC). The optical spectra were obtained at the William Herschel Telescope at the Observatory of the Roque de los Muchachos operated by the Royal Greenwich Observatory.

REFERENCES

Avni Y., Bachall J. N., 1980, ApJ, 235, 694

Baldwin J. A., Philips M. M., Terlevich R. J., 1981, PASP, 93, 5

Boyle B. J., Griffiths R. E., Shanks T., Stewart G. C., Georgantopoulos I. G., 1993, MNRAS, 260, 49

Boyle B. J., Shanks T., Stewart G. C., Georgantopoulos I. G., Griffiths R. E., 1994, MNRAS, in press

Broadhurst T. J., Ellis R. S., Shanks T., 1988, MNRAS 235, 827

Fabbiano G., 1989, Ann. Rev. A&A., 27, 87

Filippenko A. V., Terlevich R.J., 1992, ApJ, 397, L79

Fruscione A., Griffiths R. E., Mackenty J. W, 1993, in Crincarini,D. et al. eds. Observational Cosmology, ASP Conf. Ser. 51, Astron. Soc. Pacif., San Francisco, p296

Georgantopoulos I. G., Stewart G. C., Shanks T., Griffiths R. E., Boyle B. J., 1993, MNRAS, 262, 619

Georgantopoulos I. G., Stewart G. C., Shanks T., Griffiths R. E., Boyle B. J., 1994, MNRAS, submitted

Giacconi R., Gursky H., Paolini F., Rossi B. B., 1962, Phys. Rev. Lett., 9, 439

Griffiths R. E., Tuohy I. R., Brissenden R. J. V., Ward M. J., 1992, MNRAS, 255, 545

Hasinger G., Burg R., Giacconi R., Hartner G., Schmidt M., Trümper J., Zamorani G., 1993, A&A, 275, 1

Maccacaro T., Della Ceca R., Gioia I.M., Morris S.L., Stocke J.T., Wolter A, 1991, ApJ, 237, 117

McMahon R. G. 1991 in Crampton,D. ed. The Space Distribution of Quasars, ASP Conf. Ser. 21, Astron. Soc. Pacif., San Francisco, p129.

McMahon R. G., Irwin M. J., 1994, MNRAS, submitted

Stocke J. T., Morris S. L., Gioia I. M., Maccacaro T., Schild R., Wolter A., Fleming T. A., Henry J. P., 1991, ApJS, 76, 813

This paper has been produced using the Blackwell Scientific Publications TEX macros.